Shiraz University

IJVR

ISSN: 1728-1997 (Print)
ISSN: 2252-0589 (Online)

Vol. 26 No. 3 Ser. No. 92 2025

# IRANIAN JOURNAL OF VETERINARY RESEARCH

**Original Article**

# Glabridin ameliorates oxidative stress and inflammation in a bovine intestinal cell line and a colitis mouse model

**An, Y.[1]; Lu, J.[1]; Wang, X.[2]; Zhang, C.[2]; Wang, Sh.[2]; Ma, Y.[2]; Qiu, Y.[2] and Guo, Sh.[2*]**

[1]MSc Student in Animal Nutrition, Henan International Joint Laboratory of Animal Welfare and Health Breeding, Faculty of Animal Nutrition, Henan University of Science and Technology, Luoyang, 471023, China; [2]Henan International Joint Laboratory of Animal Welfare and Health Breeding, Faculty of Animal Nutrition, Henan University of Science and Technology, Luoyang, 471023, China

[*]***Correspondence:*** *Sh. Guo, Henan International Joint Laboratory of Animal Welfare and Health Breeding, Faculty of Animal Nutrition, Henan University of Science and Technology, Luoyang, 471023, China. E-mail: ShuaiGuo9322@haust.edu.cn*

10.22099/ijvr.2025.50560.7464

(Received 25 Jun 2024; revised version 3 Jun 2025; accepted 17 Jun 2025)



## Abstract

**Background:** Oxidative stress (OS) adversely affects the intestinal health and mucosal barrier function in dairy cows. Glabridin (Glab), a natural flavonoid derived from licorice, has been shown to mitigate stress-related damage due to its antioxidant properties. **Aims:** This study aims to assess the impact of Glab on OS-induced damage in the bovine immortalized cell line (BIECs-21), validate its effectiveness *in vivo*, and elucidate the underlying mechanisms. **Methods:** The *in vitro* OS model of BIECs-21 was established using 400 μM $H_2O_2$. The study evaluated cell viability, lactate dehydrogenase (LDH) activity, oxidative markers, inflammatory responses, and apoptosis in BIECs-21 under various treatment conditions. Additionally, the effects of Glab were investigated in a murine model of experimental colitis induced by dextran sulfate sodium (DSS). **Results:** Glab improved cell viability, reduced LDH release, and mitigated the adverse effects of $H_2O_2$ on total anti-oxidation capacity (T-AOC), superoxide dismutase (SOD), glutathione (GSH), and malondialdehyde (MDA) levels. qRT-PCR analysis revealed that $H_2O_2$ exposure resulted in decreased expression of nuclear factor erythroid 2-related factor 2 (*Nrf*2), superoxide dismutase 1 (*SOD*1), NADPH quinine oxidoreductase-1 (*NQO*1), and heme oxygenase-1 (*HO*-1), while it increased the expression of nuclear factor-kappa B (*NF-κB*), tumor necrosis factor-α (*TNF-α*), interleukin-6 (*IL*-6), and interleukin-8 (*IL*-8), ultimately leading to apoptosis in BIECs-21. Notably, Glab supplementation partially reversed these effects. Similar benefits of Glab were observed in a DSS-induced colitis mouse model. **Conclusion:** Glab reduces OS-induced apoptosis *in vitro* and *in vivo* by enhancing antioxidant capacity and reducing inflammation.

**Key words:** Antioxidant, Apoptosis, Glabridin, Inflammation, Oxidative stress

## Introduction

Reactive oxygen species (ROS) are byproducts of aerobic metabolism with positive effects on cells and the immune system at low to moderate levels, but excessive production can induce oxidative stress (OS) and pro-inflammatory responses, resulting in lipid peroxidation, protein oxidation, and DNA damage (Kong *et al*., 2018). These detrimental effects are significant contributors to the development of diseases. Lactation initiation, parturition, and late pregnancy metabolic demands in dairy cows are expected to induce an elevation in the production of ROS, consequently resulting in OS (Qiao *et al*., 2024). This, in turn, may have detrimental effects on the cows' overall welfare, milk production, reproductive and ultimately performance, and ultimately leads to a decrease in the profitability of the dairy industry (Surai *et al*., 2019). The intestines, as the largest organ of the immune system, play a crucial role in digestion, nutrient absorption, and pathogen defense (Choi *et al*., 2022). Given its high metabolic rate, the intestine is vulnerable to OS, which can cause damage to the intestinal epithelial barrier, leading to pathogenic bacterial invasion and inflammation (Lin *et al*., 2020). Intestinal epithelial cells are essential to maintaining the intestinal barrier (Qiu *et al*., 2021), so it's necessary to identify an effective approach to alleviate OS-induced damage in bovine intestinal epithelial cells (BIECs).

The level of OS depends on the balance between ROS production and antioxidant defenses. Medicinal plants' flavonoids may alleviate OS by regulating antioxidant defense (Sun *et al*., 2017). Glabridin (Glab) is a flavonoid compound extracted from licorice (*Glycyrrhiza glabra*) with antioxidant and anti-inflammatory properties (Simmler *et al*., 2013). Prior research has established that oral administration of Glab safeguards low-density lipoprotein from oxidation (Carmeli and Fogelman, 2009). The protective effects of Glab on chondrocytes from OS and apoptosis, as well as its promotion of mTOR-mediated autophagy, have been shown to inhibit the development of osteoarthritis in rats (Dai *et al*., 2021). Additionally, Glab has been

demonstrated to alleviate carbon tetrachloride-induced inflammation and OS in mice (Zhang *et al*., 2022). Nevertheless, the potential regulatory effect of Glab on OS in BIECs remains to be elucidated.

This study investigated Glab's ability to mitigate oxidative damage in BIECs-21 and assessed the *in vivo* effects in a mouse model of dextran sodium sulfate (DSS)-induced colitis. Additionally, the underlying mechanisms were explored. Our findings will support new dietary strategies to protect dairy cows from the adverse effects of OS.

## Materials and Methods

### Ethical statement

This study was approved by the Experimental Animals Committee of Henan University of Science and Technology (approval No.: 2023086). The code of ethics complies with European Commission standards.

### Screening the optimal concentration of $H_2O_2$ and Glab

The bovine immortalized cell line (BIECs-21) was chosen for *in vitro* studies and cultured as described by Meng *et al*. (2023). Upon reaching 80% confluence, $H_2O_2$ was applied to the cells at different concentrations for 4 h (0, 200, 400, 600, 800, and 1000 μM), or treated with varying concentrations of Glab (0, 0.01, 0.1, 1, 5, and 10 μM) for 24 h (each with six replicas). Post-treatment, the medium was replaced with fresh medium containing 10% cell counting kit-8 reagent (CCK-8; Solarbio, Beijing, China) and incubated at 37°C for 2 h. Absorbance at 450 nm was measured using a Thermo Fisher microplate reader (Waltham, MA, USA), and cell viability was calculated using the formula:

$$\text{Viability (\%)} = [(A_{sample} - A_{blank})/(A_{control} - A_{blank})] \times 100$$

where,
A: The average absorbance at 450 nm

### Experimental grouping

When the cells reached 70-80% confluence, they were divided into four groups (each with six replicas):
(1) Complete medium-incubated control cells
(2) Glab group incubated with 0.1 μmol/L of Glab
(3) OS group incubated with complete medium for 20 h followed by 4 h with 400 μmol/L of $H_2O_2$
(4) Glab+OS group incubated with 0.1 μmol/L of Glab for 20 h followed by 4 h with 400 μmol/L of $H_2O_2$

### Effect of Glab on viability and lactate dehydrogenase (LDH) activity of BIECs-21 subjected to OS

Cells were seeded at $2\times10^3$ per well in 96-well plates, and viability was measured using the CCK-8 assay with absorbance read at 450 nm. BIECs-21 were seeded at $4 \times 10^5$ cells per well in 6-well plates, and LDH activity in the supernatants was measured using a commercially available kit (Nanjing Jiancheng Bioengineering Inst., Nanjing, China) following the manufacturer's directions.

### Apoptosis assay with Annexin V-FITC/Propidium Iodide (PI)

Cells were seeded at $4 \times 10^5$ per well in 6-well plates. Apoptosis was assessed with an Annexin V-FITC/PI staining kit (TransGen Biotech, Beijing, China). After collection and washing with cold PBS, cells were re-suspended in 100 μL Annexin V Binding Buffer, stained with 5 μL each of Annexin V-FITC and PI, and incubated for 15 min in the dark. Then, 400 μL of Annexin V Binding Buffer was added. The cells were observed and photographed using an inverted fluorescence microscope (Olympus, Tokyo, Japan).

### Effect of Glab on oxidation-related indexes in BIECs-21 subjected to OS

BIECs-21 were seeded at $4 \times 10^5$ cells/well in 6-well plates. The cell lysate was collected, and the levels of glutathione (GSH), total antioxidant capacity (T-AOC), malondialdehyde (MDA), and superoxide dismutase (SOD) activity were measured using commercially available kits (Nanjing Jiancheng Bioengineering Inst., Nanjing, China).

### Gene expression analysis by quantitative RT-PCR (qRT-PCR)

Total RNA was extracted using TRIzol reagent (Solarbio, Beijing, China). The concentration and purity were evaluated using a Nanodrop ND-2000 spectrophotometer (Thermo Fisher Scientific, Wilmington, NC, USA). The RNA underwent reverse transcription into cDNA with the HiScript III RT SuperMix 100 for qPCR (+gDNA wiper) kit (Vazyme, Nanjing, China). qRT-PCR was performed using the ChamQ Universal SYBR qPCR Master Mix kit (Vazyme, Nanjing, China). β-actin was used as the internal reference gene, and the relative mRNA expression levels were calculated using the $2^{-\Delta\Delta Ct}$ method. Primer sequences and PCR product sizes are listed in Table 1.

### Experimental grouping of animals

Female Kunming mice (6-8 weeks old, 20.0±2.0 g) were obtained from Luoyang Frontier Biotechnology Co. The mice were housed in plastic cages (12 h dark/light cycle) with standard pellet diets and fed water freely. Following a week of acclimatization, they were used for the experiments. Four groups of mice were randomly assigned as described below (each with six replicas). We examined the effects of Glab on mice with experimental colitis induced by DSS (Sotillo *et al*., 2017). Glab was administered via oral gavage at a fixed daily time. The treatment protocols were as follows: control group, Glab group (20 mg/kg/day for 7 days), DSS group (normal water for 7 days followed by 3.5% DSS for 7 days), and Glab+DSS group (20 mg/kg/day Glab for 7 days followed by 3.5% DSS for 7 days). At the end of the experiment, the mice with colitis developed fecal blood.

**Table 1:** Primer sequences and amplicon sizes for qRT-PCR in BIECs-21

| Gene | Accession No. | Primer sequence（5′→3′） | Length (bp) |
|---|---|---|---|
| *Nrf*2 | NM-001011678.2 | F: AGCCTCAAAGCACCGTCC<br>R: ATCAAATCCATGTCCTGCTGGG | 87 |
| *SOD*1 | NM-174615.2 | F: CACCATCCACTTCGAGGCAA<br>R: GCACTGGTACAGCCTTGTGT | 126 |
| *NQO*1 | NM-001034535.1 | F: CTCTGGCCAATTCAGAGTGG<br>R: GGGAGTGTGCCCAATGCTAT | 87 |
| *HO*-1 | NM-001014912.1 | F: ATCGACCCCACACCTACACA<br>R: GACGCCATCACCAGCTTAAAAC | 189 |
| *NF-κB* | BC133594.1 | F: GAGGACATTCAGAGGGCAGG<br>R: CGGCTTTGATGGGTCATCCT | 192 |
| *TNF-α* | NM-173966.3 | F: TGCCTTGGCTCAGATGTGTT<br>R: GAGCGGAGGTTCAGTGATGT | 181 |
| *IL*-6 | NM-173923.2 | F: TTCACAAGCGCCTTCACTCC<br>R: GCGCTTAATGAGAGCTTCGG | 165 |
| *IL*-8 | JN559767.1 | F: CGAGGTCTGCTTAAACCC<br>R: CCCACACAGTACATGAGGC | 197 |
| *Bax* | NM-173894.1 | F: GGCCCTTTTGCTTCAGGGT<br>R: CACAGCTGCGATCATCCTCT | 181 |
| *Bcl*-2 | NM-001166486.1 | F: TGGCCTTCTTTGAGTTCGGAG<br>R: ATACAGCTCCACAAAGGCGTC | 164 |
| *Cas*-9 | NM-001205504.2 | F: AGAGACTCGAGGGAGTCAGG<br>R: CGGCTTTGATGGGTCATCC | 127 |
| *Cas*-3 | XM-019953295.1 | F: AGTCAGTCAGTTGGGCACTC<br>R: CACACCCGTAGCTGTGAAGA | 146 |
| *β-actin* | NM-173979.3 | F: CCGCAACCAGTTCGCCAT<br>R: AGGGTCAGGATGCCTCTCTT | 216 |

**Table 2:** The sequences of mouse primers for qRT-PCR

| Gene | Accession No. | Primer sequence（5′→3′） | Length (bp) |
|---|---|---|---|
| *Nrf*2 | NM-010902.5 | F: AGCGACAGAAGGACTATGAGC<br>R: TATCCAGGGCAAGCGACTCA | 297 |
| *SOD*1 | NM-011434.2 | F: GTCCGTCGGCTTCTCGTCTT<br>R: TTCACCGCTTGCCTTCTGCT | 154 |
| *NQO*1 | NM-008706.5 | F: CTACGCCATGAAGGAGGCTG<br>R: ACCACTGCAATGGGAACTGAAA | 263 |
| *HO*-1 | NM-010442.2 | F: GCCTCCAGAGTTTCCGCATA<br>R: AGGAAGCCATCACCAGCTTAAA | 275 |
| *NF-κB* | AF069542.1 | F: AAGGCCCAGGCGGATATCTA<br>R: AATCCTGGCTGACTCATGGC | 156 |
| *TNF-α* | NM-001278601.1 | F: CCCTCACACTCACAAACCAC<br>R: ACAAGGTACAACCCATCGGC | 133 |
| *IL*-6 | NM-001314054.1 | F: GACAAAGCCAGAGTCCTTCAGA<br>R: TGTGACTCCAGCTTATCTCTTGG | 76 |
| *IL*-8 | NM-011339.2 | F: CTAGGCATCTTCGTCCGTCC<br>R: CAGAAGCTTCATTGCCGGTG | 282 |
| *Bax* | NM-007527.4 | F: ATGGAGCTGCAGAGGATGAT<br>R: CAGCCACCCTGGTCTTGGA | 254 |
| *Bcl*-2 | NM-009741.5 | F: CGTCGTGACTTCGCAGAGAT<br>R: TAGTTCCACAAAGGCATCCCAG | 279 |
| *Cas*-9 | NM-015733.5 | F: GGGAAGCCCAAGCTCTTCTT<br>R: CCAGGAGACAAAACCTGGGAA | 234 |

| | | | |
|---|---|---|---|
| *Cas*-3 | NM-001284409.1 | F: GAGCTTGGAACGGTACGCTA<br>R: GCGAGATGACATTCCAGTGC | 224 |
| *β-actin* | AY618569.1 | F: AGCTGAGAGGGAAATCGTGC<br>R: CTTCTCCAGGGAGGAAGAGGA | 106 |

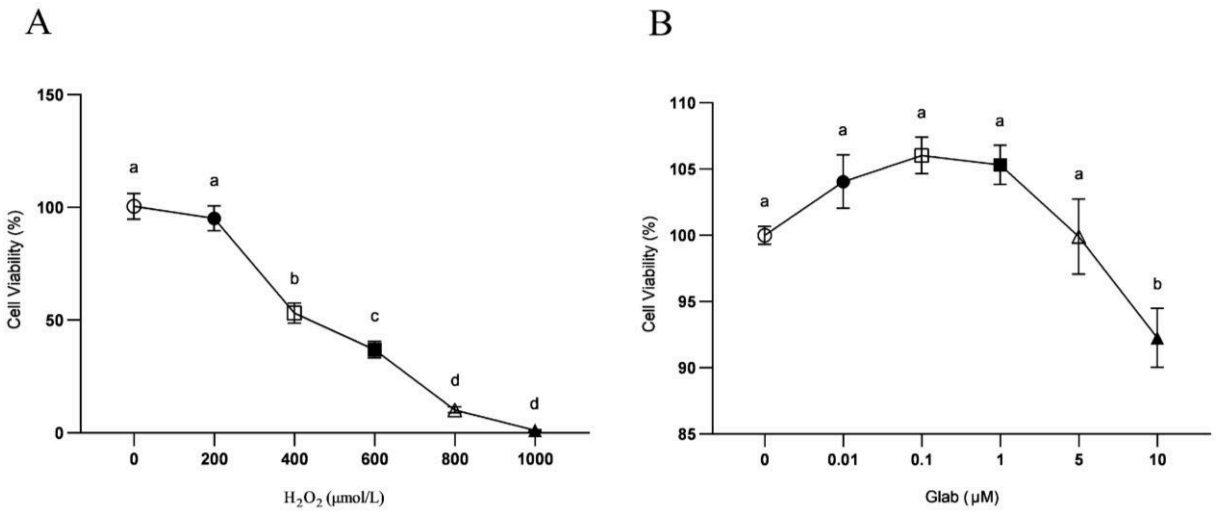


**Fig. 1:** Effect of (**A**) $H_2O_2$ and (**B**) Glab on the viability of BIECs-21. Data are mean±SEM (n=6), and different letters indicate significant differences (P<0.05)

Following the anesthesia with isoflurane, colon samples were collected and frozen at -80°C. All experimental procedures were conducted in accordance with the institutional ethical guidelines.

### qRT-PCR analysis of tissue gene expression

As mentioned earlier, qRT-PCR was used to detect gene expression in mouse colon tissue. PCR primer sequences and product sizes are listed in Table 2.

### Statistical analysis

Data were presented as mean±SEM. Comparisons between groups were conducted using IBM SPSS 19.0 software, and the results were presented graphically using GraphPad Prism 8.0. One-way ANOVA with Duncan test was used to analyze the effects of varying concentrations of $H_2O_2$ and Glab on cell activity. The Student's t-test was used for other indicators. P<0.05 indicates a significant statistical difference.

## Results

### The optimal concentration of $H_2O_2$ and Glab

The viability of cells decreased dose-dependently as shown in Fig. 1A. Notably, a significant reduction of approximately 50% in cell viability was observed at 400 μM. In Fig. 1B, cell viability was higher at 0.01-1 μM but lower at 5-10 μM compared to the control group. The 0.1 μM Glab group had the highest cell viability.

### Effect of Glab on viability and LDH activity of BIECs-21 subjected to OS

Figure 2A shows no significant difference between the Glab and control groups for cell viability (P>0.05), while the OS group had significantly reduced cell viability (P<0.001). The viability of the Glab+OS group was significantly higher than the OS group (P<0.01). In Fig. 2B, there was no significant difference in LDH activity between the Glab and control group (P>0.05), but the OS group activity was significantly higher than control (P<0.001). The Glab+OS group had lower LDH activity than the OS group (P<0.05).

### Effect of Glab on apoptosis of BIECs-21 subjected to OS

In Fig. 3, the control group had few Annexin V-FITC and PI-positive cells, while the OS group had significantly more. The Glab+OS group had fewer positive cells compared to the OS group.

### Effect of Glab on oxidation-related indexes of BIECs-21 subjected to OS

As depicted in Fig. 4, the Glab group had higher antioxidant levels and lower MDA levels compared to the control group. BIECs-21 under OS had decreased antioxidant levels and increased MDA levels. The Glab+OS group had higher antioxidant levels and lower MDA levels compared to the OS group.

### Effect of Glab on the expression of antioxidation genes

Table 3 indicates that the Glab group had significantly higher mRNA levels of nuclear factor erythroid 2-related factor 2 (*Nrf*2; P<0.05), superoxide dismutase 1 (*SOD*1; P<0.001) and heme oxygenase-1 (*HO*-1; P<0.001) compared to the control, Glab had no significant effect on NADPH quinine oxidoreductase-1 (*NQO*1; P>0.05). Conversely, the expression levels of

these genes were significantly lower in the OS group. The Glab+OS group showed a significant increase in *Nrf*2, *NQO*1, and *HO*-1 expression compared to the OS group. Table 4 shows that the Glab group mice exhibited a significantly higher expression of *Nrf*2, *NQO*1 compared to the control, while the DSS group had significantly decreased levels of *NQO*1, *HO*-1. The Glab+DSS group demonstrated significantly higher expression levels of *Nrf*2, *SOD*1 and *NQO*1 when compared to the DSS group.

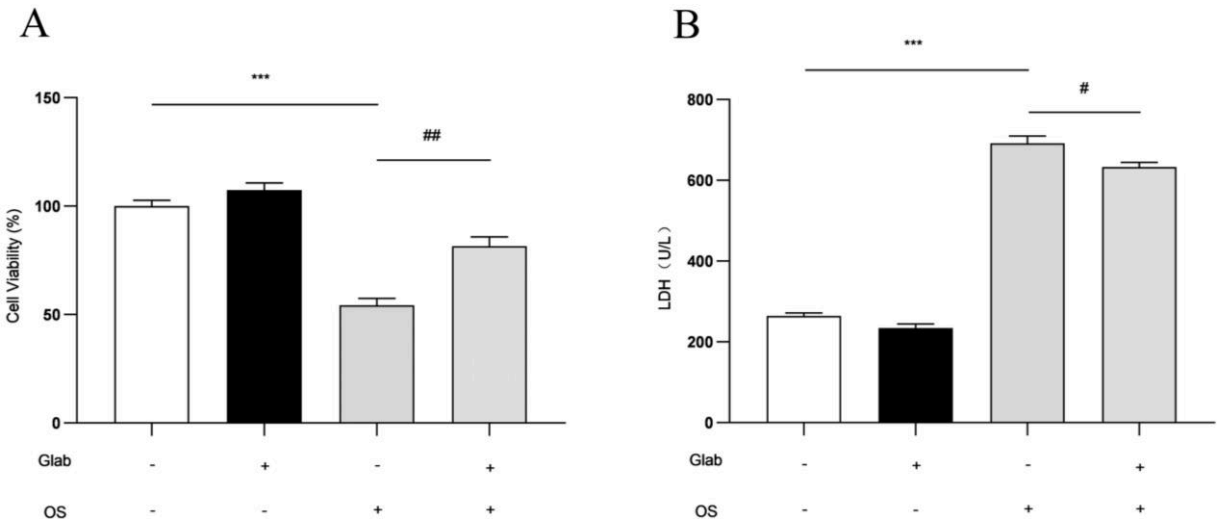


**Fig. 2:** Effect of (**A**) Glab on viability and (**B**) LDH activity of BIECs-21 subjected to OS. Data are mean±SEM (n=6). The Glab group and the OS group were compared with the control (* P<0.05, ** P<0.01, *** P<0.001). Additionally, we compared the Glab+OS and the OS groups (# P<0.05, ## P<0.01, ### P<0.001)

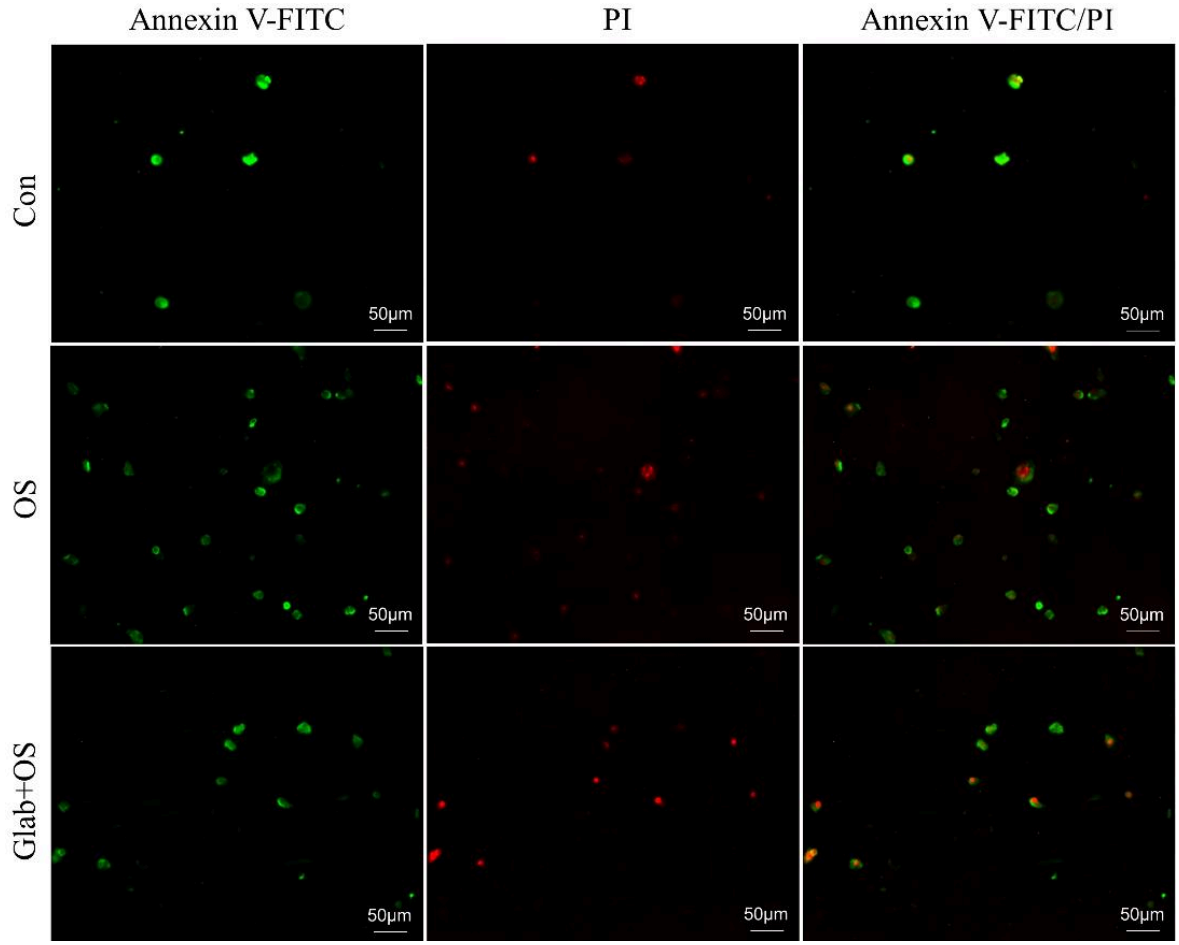


**Fig. 3:** Effect of Glab on apoptosis of BIECs-21 subjected to OS. The green spots correspond to Annexin V-FITC+ cells, whereas the red spots correspond to PI+ cells, (scale bar, 50 μm)

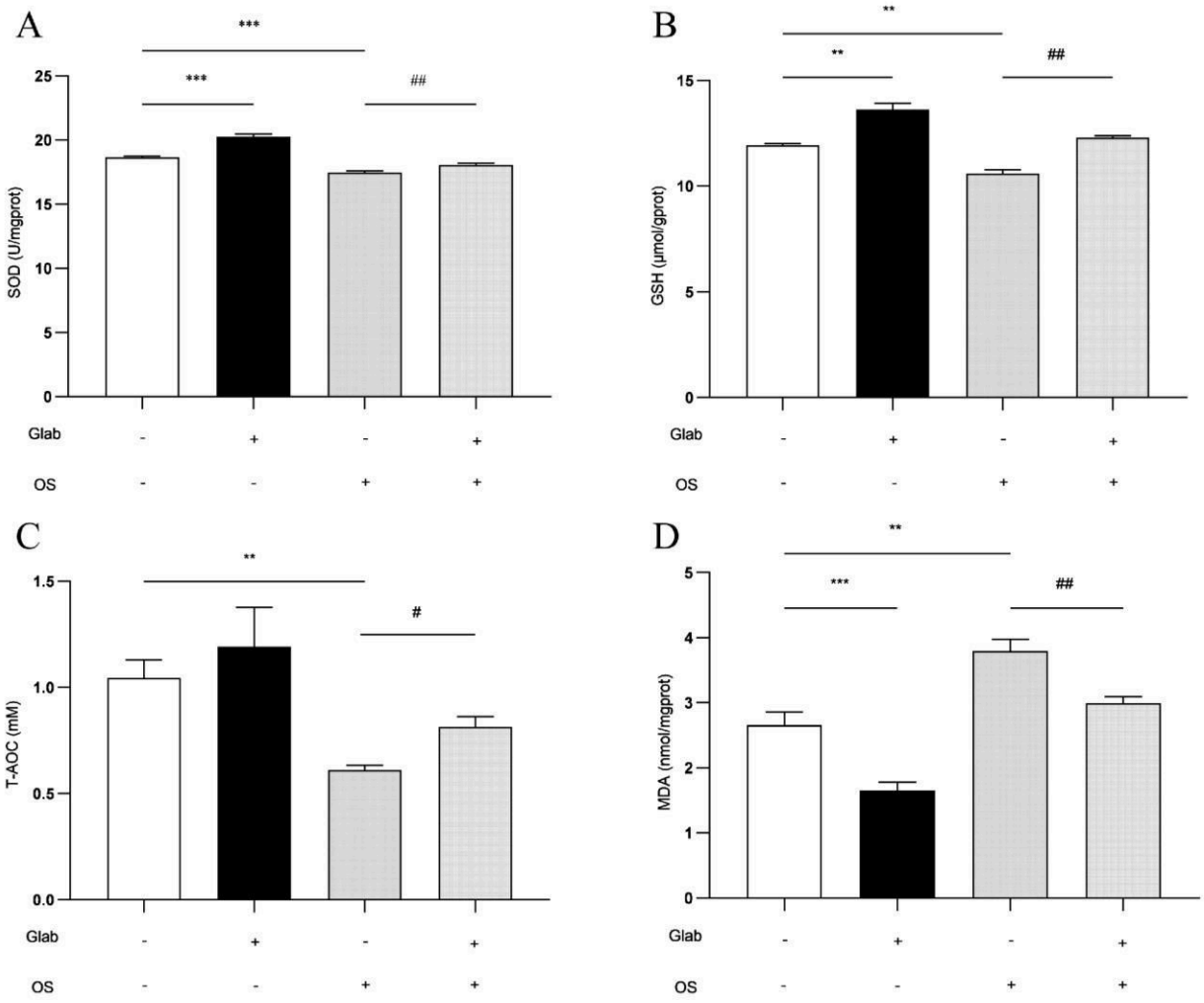


**Fig. 4:** Effect of Glab on oxidation-related indexes in BIECs-21 subjected to OS. (**A**) SOD: superoxide dismutase, (**B**) GSH: glutathione, (**C**) T-AOC: total antioxidant capacity, and (**D**) MDA: malondialdehyde. Data are mean±SEM (n=6). The Glab group and the OS group were compared with the control (* P<0.05, ** P<0.01, *** P<0.001). Additionally, we compared the Glab+OS and the OS groups (# P<0.05, ## P<0.01, ### P<0.001)

**Table 3:** Effect of Glab on gene expression in BIECs-21 subjected to OS

| Item | Con | Glab | OS | Glab+OS |
|---|---|---|---|---|
| *Nrf*2 | 1.00±0.04 | 1.11±0.02$^{*}$ | 0.50±0.02$^{***}$ | 0.85±0.02$^{###}$ |
| *SOD*1 | 1.00±0.03 | 1.41±0.05$^{***}$ | 0.89±0.02$^{*}$ | 0.97±0.02 |
| *NQO*1 | 1.00±0.02 | 1.06±0.01 | 0.46±0.01$^{***}$ | 0.67±0.07$^{#}$ |
| *HO*-1 | 1.00±0.02 | 1.25±0.03$^{***}$ | 0.58±0.01$^{***}$ | 1.09±0.01$^{###}$ |
| *NF-κB* | 1.03±0.11 | 0.75±0.04 | 1.25±0.05 | 0.84±0.04$^{##}$ |
| *TNF-α* | 1.00±0.06 | 0.61±0.08$^{*}$ | 1.10±0.07 | 0.69±0.12$^{#}$ |
| *IL*-6 | 1.00±0.04 | 0.86±0.02 | 1.34±0.02$^{**}$ | 0.73±0.01$^{###}$ |
| *IL*-8 | 1.00±0.02 | 0.79±0.01$^{***}$ | 1.12±0.02$^{**}$ | 0.96±0.04$^{#}$ |
| *Bax* | 1.00±0.06 | 0.96±0.02 | 1.22±0.01$^{**}$ | 0.87±0.01$^{###}$ |
| *Bcl*-2 | 1.02±0.11 | 1.18±0.15 | 0.67±0.05$^{*}$ | 1.31±0.05$^{###}$ |
| *Cas*-9 | 1.00±0.02 | 0.85±0.03$^{*}$ | 1.45±0.07$^{***}$ | 0.63±0.04$^{###}$ |
| *Cas*-3 | 1.01±0.05 | 0.94±0.03 | 1.61±0.04$^{***}$ | 1.16±0.03$^{###}$ |
| *Bcl*-2/*Bax* | 1.02±0.13 | 1.22±0.14 | 0.55±0.04$^{**}$ | 1.50±0.06$^{###}$ |

Data are mean±SEM (n=6). The Glab group and the OS group were compared with the control (* P<0.05, ** P<0.01, *** P<0.001). Additionally, we compared the Glab+OS and the OS groups (# P<0.05, ## P<0.01, ### P<0.001)

**Table 4:** Effect of Glab on gene expression in DSS-induced colitis mice

| Item | Con | Glab | DSS | Glab+DSS |
|---|---|---|---|---|
| *Nrf*2 | 1.03±0.16 | 1.99±0.18$^{*}$ | 0.73±0.04 | 1.62±0.10$^{##}$ |
| *SOD*1 | 1.04±0.19 | 1.71±0.16 | 0.64±0.01 | 1.82±0.03$^{###}$ |
| *NQO*1 | 1.01±0.09 | 1.38±0.06$^{*}$ | 0.61±0.07$^{*}$ | 1.37±0.10$^{#}$ |

| | | | | |
|---|---|---|---|---|
| *HO*-1 | 1.01±0.14 | 1.17±0.06 | 0.52±0.03** | 0.65±0.10 |
| *NF-κB* | 1.01±0.09 | 0.86±0.08 | 1.39±0.09* | 0.94±0.06# |
| *TNF-α* | 1.03±0.15 | 0.72±0.05 | 1.57±0.06* | 0.91±0.08## |
| *IL*-6 | 1.00±0.05 | 0.70±0.04* | 1.64±0.05* | 1.16±0.07# |
| *IL*-8 | 1.00±0.02 | 0.64±0.12 | 1.50±0.05** | 1.18±0.08# |
| *Bax* | 1.04±0.12 | 0.73±0.04 | 1.90±0.09* | 0.77±0.08## |
| *Bcl*-2 | 1.00±0.06 | 1.10±0.05 | 0.64±0.04** | 1.25±0.05## |
| *Cas*-9 | 1.02±0.12 | 0.80±0.14 | 1.58±0.10* | 0.69±0.12## |
| *Cas*-3 | 1.03±0.16 | 0.72±0.11 | 1.55±0.09* | 1.00±0.13# |
| *Bcl*-2/*Bax* | 0.98±0.05 | 1.52±0.15* | 0.34±0.03*** | 1.64±0.18## |

Data are mean±SEM (n=6). The Glab group and the DSS group were compared with the control (* P<0.05, ** P<0.01, *** P<0.001). Additionally, we compared the Glab+DSS and the DSS groups (# P<0.05, ## P<0.01, ### P<0.001)

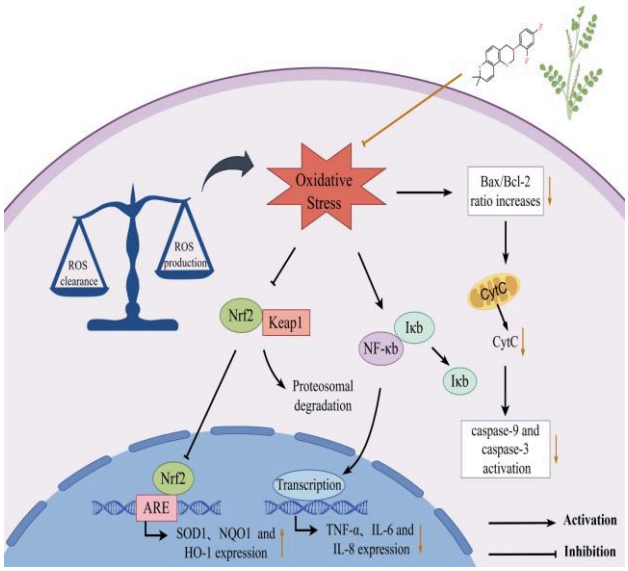


**Fig. 5:** Possible mechanism diagram of Glab reducing OS damage (figure fodder by Figdraw). Glab reduces OS-induced damage in BIECs-21 by activating *Nrf2* and inhibiting *NF-κB* signaling

## Effect of Glab on expression of inflammatory factors genes

Table 3 data indicates that the Glab group had significantly lower levels of tumor necrosis factor-alpha (*TNF-α*; P<0.05) and interleukin-8 (*IL*-8; P<0.001) compared to control, Glab had no significant effect on nuclear factor-kappa B (*NF-κB*) and interleukin-6 (*IL*-6). Conversely, the expression levels of *IL*-6 and *IL*-8 were significantly higher in the OS group. The Glab+OS group showed significantly decreased levels compared to the OS group. As shown in Table 4, the Glab group mice exhibited a significantly lower expression of *IL*-6 compared to the control group, while the DSS group had significantly increased levels of pro-inflammatory genes. Pretreatment with Glab significantly lowered pro-inflammatory gene expression compared to DSS treatment alone.

## Effect of Glab on the expression of apoptosis genes

Table 3 indicates that the Glab group showed significantly increased levels of Caspase-9 (*Cas*-9; P<0.05) compared to control, Glab had no significant effect on *Bcl*-2-associated X (*Bax*), Caspase-3 (*Cas*-3), B-cell lymphoma-2 (*Bcl*-2), and *Bcl*-2/*Bax* ratio. The OS group showed significantly increased levels of *Bax*, *Cas*-3, and *Cas*-9, as well as significantly decreased levels of *Bcl*-2 and *Bcl*-2/*Bax* ratio compared to the control. In the Glab+OS group, levels of *Bax*, *Cas*-3, and *Cas*-9 were significantly lower than in the OS group, while levels of *Bcl*-2 and the *Bcl*-2/*Bax* ratio were significantly higher. Table 4 shows that Glab significantly increased the *Bcl*-2/*Bax* ratio compared to the control. DSS treatment led to significant upregulation of *Bax*, *Cas*-3, and *Cas*-9, and significant downregulation of *Bcl*-2 and the *Bax*/*Bcl*-2 ratio. Compared to the DSS group, *Bax*, *Cas*-3, and *Cas*-9 expression decreased significantly in the Glab+DSS group, while *Bcl*-2 expression and the *Bax*/*Bcl*-2 ratio increased significantly. The above results indicate that Glab exhibits superior antioxidant and anti-inflammatory characteristics, which can effectively reduce cellular damage and inhibit apoptosis *in vitro* and *in vivo*. Figure 5 illustrates a possible mechanism.

## Discussion

After 4 h of exposure to 400 μM $H_2O_2$, BIECs-21 viability decreased by approximately 50%, in agreement with previous research (Mei *et al*., 2021). Thus, this concentration and duration were chosen to create an OS model *in vitro*. Glab exhibited a beneficial impact on cell viability at concentrations below 5 μM, with the highest level observed at 0.1 μM, which was chosen for further experiments.

Cell viability is an essential metric that indicates the normal proliferation of cells under specific conditions. The present investigation observed a significant reduction in cell viability after subjecting BIECs-21 to a 4 h incubation with 400 μM $H_2O_2$. Nevertheless, pre-treatment with 0.1 μM Glab effectively mitigated this decline, indicating a substantial improvement in the overall state of the cell. Excessive ROS production induces cell damage and death, releasing LDH into the cell culture (Wesdorp *et al*., 2023). This study found that pretreatment with Glab led to a decrease in LDH activity compared to the OS group, suggesting a potential protective effect against OS-induced membrane damage.

The cellular antioxidant defense system, including SOD and GSH, is essential for detoxifying ROS and maintaining cellular function (Jiang *et al*., 2021). Previous studies revealed that licorice's total flavonoids exhibit anti-lipid peroxidation properties, leading to a

reduction in MDA production (Gao *et al*., 2022). Additionally, the supplementation of licorice flavonoids in the diet of mice was found to elevate the levels of T-AOC in both blood and liver tissue (Du *et al*., 2022). This study indicated that pretreatment with Glab resulted in elevated SOD activity, GSH levels, T-AOC levels, and decreased MDA levels compared to the OS group, suggesting that Glab enhances antioxidant capacity and alleviates the extent of OS-induced injury.

The cytoplasmic kelch-like ECH-associated protein 1 (*Keap*1) binds to *Nrf*2 to regulate oxidative balance. When OS occurs, *Nrf*2 moves to the nucleus to activate antioxidant genes, preventing ROS accumulation (Koh *et al*., 2018). However, excessive OS can result in oxidative damage to intracellular biomolecules, aberrant gene expression, DNA structural alterations, and disruption of essential intercellular signaling pathways (Zheng *et al*., 2022). OS suppressed *Nrf*2 and its target genes, but Glab pretreatment reversed this effect, indicating Glab's protective role against OS by regulating anti-oxidative gene expression. Studies have shown that oral administration of Glab at doses ranging from 5 to 20 mg/kg protects the liver from paracetamol-induced damage (Bhatt *et al*., 2022). The use of 20 and 30 mg/kg effectively alleviated pulmonary dysfunction and inflammation in an asthma mouse model (Dogan *et al*., 2020). During this study, the oral dose was set at 20 mg/kg/day. DSS can compromise the intestinal epithelial barrier, allowing antigens and microbes to penetrate the mucosa, thereby activating an inflammatory response (Chao *et al*., 2020). Emerging evidence indicates that inflammation triggers OS by enhancing ROS generation (Shao *et al*., 2023). Consequently, a mouse model of experimental colitis induced by DSS was used to evaluate the efficacy of Glab *in vivo*. Our findings demonstrated that Glab possesses the ability to increase the antioxidant capacity of intestinal cells during the inflammatory state.

*NF-κB* is one of the most important transcription factors involved in inflammation. Under normal conditions, inactive *NF-κB* is sequestered in the cytoplasm by binding to *IκB* proteins (Wang *et al*., 2020). Elevated levels of ROS can trigger *NF-κB* phosphorylation, facilitating its nuclear translocation, where it transcribes pro-inflammatory genes (Leathem *et al*., 2022). Studies have found that Licorice flavone can reduce inflammation by affecting the *NF-kB/MAPK* pathway (Shawky *et al*., 2020). In this study, pretreatment with Glab reduced the expression of *NF-κB* and inflammatory genes in BIECs-21 exposed to OS. These findings suggest that Glab possesses the ability to suppress inflammatory responses triggered by OS. *In vitro* experiments demonstrated that Glab inhibits the *NF-κB* signaling pathway and improves symptoms of mice with DSS-induced colitis.

Furthermore, excessive accumulation of ROS can disrupt cell structure and function, ultimately culminating in apoptotic cell death, thereby triggering cell loss and inducing tissue injury (Jafri and Kumar, 2014). *Bcl*-2 and *Bax* proteins control mitochondrial membrane permeability, influencing apoptosis initiation by regulating cytochrome c release (Kim *et al*., 2021). *Bax* increases membrane permeability, allowing cytochrome c to enter the cytosol and trigger caspase activation, leading to cell death (Yang *et al*., 2015). *Bcl*-2 has the opposite effect, indicating resistance or susceptibility to apoptosis based on its levels compared to *Bax*. In this study, notable upregulation of *Bax*, *Cas*-3, and *Cas*-9 expression was observed in the BIECs-21 OS model, while the levels of *Bcl*-2 genes and *Bcl*-2/*Bax* ratio showed a decline. Notably, Glab effectively mitigated apoptosis induced by OS. qRT-PCR results were supported by Annexin V-FITC/PI staining. Inflammation progression leads to OS and causes apoptosis through more direct mechanisms (Ni *et al*., 2015). We found that Glab had a protective effect on intestinal cell apoptosis in colitis induced by DSS in mice by increasing anti-apoptotic genes and decreasing pro-apoptotic genes.

The findings of this study demonstrate Glab's efficacy in reducing oxidative damage to BIECs-21, which may be due to the augmentation of antioxidant capabilities and modulation of inflammatory cytokine production. Additionally, Glab exhibits a beneficial impact on antioxidant levels in a murine model of colitis. Thus, Glab may be a promising dietary supplement for preventing and mitigating OS-induced intestinal damage.

## Acknowledgements

We are grateful to all laboratory members for their support during this study. This research was funded by the National Key Research and Development Program of China (2022YFE0111100) and the Program for International S&T Cooperation Projects of Henan (232102521012).

## Conflict of interest

The authors declare no competing interests.

## References

**Bhatt, S; Sharma, A; Dogra, A; Sharma, P; Kumar, A; Kotwal, P; Bag, S; Misra, P; Singh, G; Kumar, A; Sangwan, PL and Nandi, U** (2022). Glabridin attenuates paracetamol-induced liver injury in mice via CYP2E1-mediated inhibition of oxidative stress. Drug Chem. Toxicol., 45: 2352-2360.

**Carmeli, E and Fogelman, Y** (2009). Antioxidant effect of polyphenolic glabridin on LDL oxidation. Toxicol. Ind. Health. 25: 321-324.

**Chao, L; Li, Z; Zhou, J; Chen, W; Li, Y; Lv, W; Guo, A; Qu, Q and Guo, S** (2020). Shen-Ling-Bai-Zhu-San improves dextran sodium sulfate-induced colitis by inhibiting caspase-1/caspase-11-mediated pyroptosis. Front. Pharmacol., 11: 814.

**Choi, J; Kim, BR; Akuzum, B; Chang, L; Lee, JY and Kwon, HK** (2022). T(REG)king from gut to brain: the control of regulatory T cells along the gut-brain axis. Front.

Immunol., 13: 916066.

**Dai, J; Zhang, Y; Chen, D; Chen, D; Li, X; Wang, J and Sun, Y** (2021). Glabridin inhibits osteoarthritis development by protecting chondrocytes against oxidative stress, apoptosis and promoting mTOR mediated autophagy. Life Sci., 268: 118992.

**Dogan, MF; Parlar, A; Cam, SA; Tosun, EM; Uysal, F and Arslan, SO** (2020). Glabridin attenuates airway inflammation and hyperresponsiveness in a mice model of ovalbumin-induced asthma. Pulm. Pharmacol. Ther., 63: 101936.

**Du, J; Cao, L; Gao, J; Jia, R; Zhu, H; Nie, Z; Xi, B; Yin, G; Ma, Y and Xu, G** (2022). Protective effects of glycyrrhiza total flavones on liver injury induced by streptococcus agalactiae in tilapia (*Oreochromis niloticus*). Antibiotics (Basel). 11: 1648.

**Gao, Z; Wang, Y and Yu, H** (2022). A chinese classical prescription chaihu shugan powder in treatment of post-stroke depression: an overview. Medicina (Kaunas). 59: 55.

**Jafri, MS and Kumar, R** (2014). Modeling mitochondrial function and its role in disease. Prog. Mol. Biol. Transl. Sci., 123: 103-125.

**Jiang, L; Gong, Y; Rao, J; Yang, Q; Gao, N; Li, G and Ma, Y** (2021). 1-O-Hexyl-2,3,5-trimethylhydroquinone ameliorates the development of preeclampsia through suppression of oxidative stress and endothelial cell apoptosis. Oxid. Med. Cell. Longev., 2021: 8839394.

**Kim, SY; Cha, HJ; Hwangbo, H; Park, C; Lee, H; Song, KS; Shim, JH; Noh, JS; Kim, HS; Lee, BJ; Kim, S; Kim, GY; Jeon, YJ and Choi, YH** (2021). Protection against oxidative stress-induced apoptosis by fermented sea tangle (*Laminaria japonica* Aresch) in osteoblastic MC3T3-E1 cells through activation of Nrf2 signaling pathway. Foods. 10: 2807.

**Koh, ES; Kim, S; Kim, M; Hong, YA; Shin, SJ; Park, CW; Chang, YS; Chung, S and Kim, HS** (2018). D-Pinitol alleviates cyclosporine A-induced renal tubulointerstitial fibrosis via activating Sirt1 and Nrf2 antioxidant pathways. Int. J. Mol. Med., 41: 1826-1834.

**Kong, SZ; Li, JC; Li, SD; Liao, MN; Li, CP; Zheng, PJ; Guo, MH; Tan, WX; Zheng, ZH and Hu, Z** (2018). Anti-aging effect of chitosan oligosaccharide on d-galactose-induced subacute aging in mice. Mar. Drugs. 16: 181.

**Leathem, A; Simone, M; Dennis, JM and Witting, PK** (2022). The cyclic nitroxide TEMPOL ameliorates oxidative stress but not inflammation in a cell model of parkinson's disease. Antioxidants (Basel). 11: 257.

**Lin, H; Chen, D; Du, Q; Pan, T; Tu, H; Xu, Y; Teng, T; Tu, J; Li, J; Lin, Z; Wang, X; Xu, L and Chen, YP** (2020). Dietary copper plays an important role in maintaining intestinal barrier integrity during alcohol-induced liver disease through regulation of the intestinal HIF-1α signaling pathway and oxidative stress. Front. Physiol., 11: 369.

**Mei, L; Zheng, Y; Ma, T; Xia, B; Gao, X; Hao, Y; Luo, Z and Huang, J** (2021). The novel antioxidant compound JSH-23 prevents osteolysis by scavenging ROS during both osteoclastogenesis and osteoblastogenesis. Front. Pharmacol., 12: 734774.

**Meng, S; Wang, YU; Wang, S; Qian, W; Shao, Q; Dou, M; Zhao, S; Wang, J; Li, M; An, Y; He, L and Zhang, C** (2023). Establishment and characterization of an immortalized bovine intestinal epithelial cell line. J. Anim. Sci., 101: skad215.

**Ni, Q; Su, X; Chen, J and Tian, W** (2015). Prediction of metabolic gene biomarkers for neurodegenerative disease by an integrated network-based approach. Biomed. Res. Int., 2015: 432012.

**Qiao, K; Jiang, R; Contreras, GA; Xie, L; Pascottini, OB; Opsomer, G and Dong, Q** (2024). The complex interplay of insulin resistance and metabolic inflammation in tansition dairy cows. Animals (Basel). 14: 832.

**Qiu, P; Liu, L; Fang, J; Zhang, M; Wang, H; Peng, Y; Chen, M; Liu, J; Wang, F and Zhao, Q** (2021). Identification of pharmacological autophagy regulators of active ulcerative colitis. Front. Pharmacol., 12: 769718.

**Shao, D; Shen, W; Miao, Y; Gao, Z; Pan, M; Wei, Q; Yan, Z; Zhao, X and Ma, B** (2023). Sulforaphane prevents LPS-induced inflammation by regulating the Nrf2-mediated autophagy pathway in goat mammary epithelial cells and a mouse model of mastitis. J. Anim. Sci. Biotechnol., 14: 61.

**Shawky, E; Nada, AA and Ibrahim, RS** (2020). Potential role of medicinal plants and their constituents in the mitigation of SARS-CoV-2: identifying related therapeutic targets using network pharmacology and molecular docking analyses. RSC Adv., 10: 27961-27983.

**Simmler, C; Pauli, GF; Chen, SN** (2013). Phytochemistry and biological properties of glabridin. Fitoterapia. 90: 160-184.

**Sotillo, J; Ferreira, I; Potriquet, J; Laha, T; Navarro, S; Loukas, A and Mulvenna, J** (2017). Changes in protein expression after treatment with *Ancylostoma caninum* excretory/secretory products in a mouse model of colitis. Sci. Rep., 7: 41883.

**Sun, Y; Lu, Q; He, L; Shu, Y; Zhang, S; Tan, S and Tang, L** (2017). Active fragment of *Veronica ciliata* fisch. attenuates t-BHP-induced oxidative stress injury in HepG2 cells through antioxidant and antiapoptosis activities. Oxid. Med. Cell. Longev., 2017: 4727151.

**Surai, PF; Kochish, II; Fisinin, VI and Juniper, DT** (2019). Revisiting oxidative stress and the use of organic selenium in dairy cow nutrition. Animals (Basel). 9: 462.

**Wang, X; Zhu, L; Hu, J; Guo, R; Ye, S; Liu, F; Wang, D; Zhao, Y; Hu, A; Wang, X; Guo, K and Lin, L** (2020). FGF21 attenuated LPS-induced depressive-like behavior via inhibiting the inflammatory pathway. Front. Pharmacol., 11: 154.

**Wesdorp, MA; Schwab, A; Bektas, EI; Narcisi, R; Eglin, D; Stoddart, MJ; Osch, GJVMV and D'Este, M** (2023). A culture model to analyze the acute biomaterial-dependent reaction of human primary neutrophils *in vitro*. Bioact. Mater., 20: 627-637.

**Yang, CH; Schrepfer, T and Schacht, J** (2015). Age-related hearing impairment and the triad of acquired hearing loss. Front. Cell. Neurosci., 9: 276.

**Zhang, L; Zhang, H; Gu, J; Xu, W; Yuan, N; Sun, J and Li, H** (2022). Glabridin inhibits liver fibrosis and hepatic stellate cells activation through suppression of inflammation and oxidative stress by activating PPARγ in carbon tetrachloride-treated mice. Int. Immunopharmacol., 113: 109433.

**Zheng, H; Zhao, Y and Guo, L** (2022). A bioactive substance derived from brown seaweeds: Phlorotannins. Mar. Drugs. 20: 742.